Title: Hydrophobic End Modulated Amino Acid Based Neutral Hydrogelators: Structure Specific Inclusion of Carbon Nanomaterials

Authors: Prasanta Kumar Das, Ph.D.; Pritam Choudhury; Deep Mandal; Sayanti Brahmachari

To be cited as: 10.1002/chem.201504888

Link to VoR: http://dx.doi.org/10.1002/chem.201504888

Hydrophobic End Modulated Amino Acid Based Neutral Hydrogelators: Structure Specific Inclusion of Carbon Nanomaterials

Pritam Choudhury, Deep Mandal, Sayanti Brahmachari and Prasanta Kumar Das*[a]

Department of Biological Chemistry, Indian Association for the Cultivation of Science, Jadavpur, Kolkata – 700 032, India

[a] P. Choudhury, D. Mandal, S. Brahmachari and Prof. P. K. Das
Department of Biological Chemistry
Indian Association for the Cultivation of Science
Jadavpur, Kolkata – 700032, India
Fax: +(91)-33-24732805
E-mail: bcpkd@iacs.res.in

*To whom correspondence should be addressed: bcpkd@iacs.res.in

Abstract

Hydrophobic end modulated L-phenylalanine containing triethylene glycol monomethyl ether tagged neutral hydogelators (**1**-**4**) were developed. Investigation was done to determine gelator's structure dependent inclusion of carbon nanomaterials (CNMs) in the self assembled fibrillar network (SAFIN). The gelators (**1**, **3** and **4**) can immobilize water and aqueous buffer (pH = 3-7) with minimum gelator concentration of 10-15 $mgmL^{-1}$. The hydrophobic part of the gelator was varied form long chain (C-16) to extended aromatic pyrenyl moiety and their ability to integrate one dimensional (1D) and two dimensional (2D) allotrope of carbon (i.e. single walled carbon nanotube (SWNT) and graphene oxide (GO), respectively) within the gel was investigated. Long alkyl chain (C-16) containing **1** can include SWNT while pyrene containing **4** can include both SWNT and GO. Gelator **3** failed to incorporate SWNT or GO due to slow rate of gelation and possibly because of mismatch between the aggregated structure and CNMs. Involvement of various forces in self-aggregated gelation and physicochemical changes occurring due to CNM inclusion were examined by spectroscopic and microscopic techniques. Distinctive pattern of self-assembly of the gelator-**1** and **4** through *J*- and *H*-type aggregation might have facilitated the structure specific CNM inclusion. Inclusion of SWNT/GO within the hydrogel matrix resulted in the reinforcement in mechanical stiffness of the composites compared to that of native hydrogels.

Introduction

The development of self assembled materials has been an expanding research area in the last few decades due to their versatile physicochemical properties as well as their mounting applications in diversified area including drug delivery, sensors, template materials and so forth.[1-6] The low molecular weight gelators (LMWG) are small organic molecules which have an ability to restrict mobility of solvents through formation of a self assembled fibrillar network (SAFIN). Gelation of small molecules is an outcome of balanced combination of various interactions such as hydrogen bonding, π–π stacking, van der Waals forces and so on. [7] An optimal balance between hydrophobicity and hydrophilicity of the amphiphile play the key role in the formation of SAFIN.[6] In recent times, the development of neutral hydrogel at physiological salinity is gaining much importance due to its suitability in bio-medicinal applications[8]. Designing of neutral hydrogelator devoid of any charged moiety that can form gel in pure water or buffer solutions at neutral pH is a very tricky task. In this context, the presence of a strong hydrophilic moiety (without any charged residue) in the gelator's structure would be the key factor towards rational designing of a neutral hydrogelator. Along with that a hydrophobic moiety and the residue capable of participating in intermolecular hydrogen bonding need to be included within the gelator's structure to maintain the required hydrophilic-lipophilic balance (HLB) for self-assembled gelation.

Simultaneously with rapid structural advancement, researchers are trying to build up soft-nanocomposites comprising of nanomaterial integrated gel with the objective to improve its physicochemical properties. Nanomaterials included hybrid gels with improved mechanical stiffness are finding applications in the area of supercapacitors, nanoelectronics, photovoltaic devices, chemical sensors, biomedicine and so on.[7a,8,9] Exogenous nanomaterials such as carbon nanotube (CNT), graphene, graphene oxide (GO), silver nanoparticle, gold nanoparticle etc. were included in the interstitial space of the SAFIN that

aided advantageous changes in their properties.[10,11] However, it is difficult to predict the inclusion of carbon nanomaterial (CNM) within the fibrillar network which may have dependence on physical dimension of the CNMs as well as on the structure of the amphiphilic gelator. Report on the gelator's structure dependent specific integration of different CNMs within SAFIN is really scarce. Distinctive structural and self-aggregation properties of gelator would play a vital role for integration of CNM within hydrogel. Hence, it would be highly intriguing to design neutral hydrogelators as well as finding a correlation between its molecular structure dependent aggregation and selective inclusion of CNMs within hydrogel matrix.

Herein, the present study reports rational designing of neutral hydrogelators comprised of hydrophobic terminal group modulated L-phenylalanine with triethylene glycol monomethyl ether (TEG) tagged hydrophilic moiety (**1**-**4**, Figure 1). Amphiphile-**1**, **3** and **4** were found to form self-assembled hydrogel in water and aqueous buffer solutions of varying pH ranging from 3.0-7.0. Amphiphile-**2** self aggregated to form gel in DMSO/water mixture (1:3 v/v). The hydrophobic end of the gelator molecule was judiciously varied from long alkyl chain (C-16) to extended aromatic pyrenyl moiety to monitor the selective CNM inclusion behaviour of hydrogels. The long chain (C-16) containing gelator-**1** efficiently disperse and include 1D allotrope of carbon, single walled carbon nanotube (SWNT) within the gel matrix. Notably, pyrene containing gelator-**4** was able to integrate both 1D and 2D allotrope of carbon (i.e. SWNT and GO) in its SAFIN. The self aggregation behaviour of the amphiphilic molecules and inclusion of different carbon nanomaterials within the SAFIN was studied by spectroscopic and microscopic means. Mechanical stiffness of the gel and CNM–gel composite was monitored by rheological study.

Results and Discussion

Development of neutral amphiphilic molecule with hydrogelation ability is of high importance. Moreover such gelator's structure dependent inclusion of CNMs within hydrogel is a very interesting research domain which has not been well explored. In this present study, we have developed neutral gelators that form hydrogel in water and aqueous buffer and tried to understand the dependence of gelator structure on specific CNM integration in its SAFIN. Accordingly, the hydrogelators (**1-4**, Figure 1, Scheme S1 and S2 in the Supporting Information) were synthesized by coupling between *C*-terminal of L-phenylalanine and twin chain hydrophilic triethylene glycol monomethyl ether (TEG) moiety attached to 2,2′-(ethylenedioxy) bis (ethylamine). The *N*-terminal of the L-phenylalanine was coupled through an amide linkage by different hydrophobic groups such as C-16 (**1**), an additional L-phenylalanine linked with C-16 (**2**), naphthalene (**3**) and pyrene (**4**). The hydrophobicity of the gelator was judiciously varied from long alkyl chain to extended aromatic group to study their aggregation pattern as well as their influence on CNMs inclusion. With the aim to develop a neutral gelator, it is essential to choose specific hydrophilic moiety that is devoid of any charge unit as well as can maintain the optimal HLB required for hydrogelation. Hence, we have chosen the TEG moiety as hydrophilic terminal. The hydrophilic TEG substituted 2,2′-(ethylenedioxy) bis (ethylamine) group enhanced the solubility of the gelator in aqueous solvents while the hydrophobicity of C-16 to pyrene might have maintained the necessary HLB for self-assembled gelation. The linker amino acid also contributed in gelation through possible intermolecular hydrogen bonding.[5,10a,b,j]

We investigated the hydrogelation efficiency of the neutral amphiphiles **1-4** in water, aqueous phosphate buffer of pH = 3-7, and DMSO-water mixture (1:3, v/v) (Table 1). Initially, amphiphile-**1**, containing C-16 alkyl chain formed gel in water having minimum gelation concentration (MGC) of 15 $mgmL^{-1}$. The formation of the gel was confirmed from

the "stable-to-inversion" of the glass vial with a diameter of 10 mm. With an expectation to improve the MGC, we have incorporated an additional L-phenylalanine to amphiphile-**2** that might help in gelation by an extra amide bond and additional aromatic residue. To our surprise, **2** did not form gel in water. However it showed efficient gelation in DMSO-water (1:3, v/v) mixture at MGC=10 $mgmL^{-1}$. Presumably, the amphiphile-**2** has lost the critical HLB required for self aggregation in water due to the presence of an extra phenyl ring compared to that of **1**. Subsequently, instead of C-16 alkyl chain, we switched to an aromatic hydrophobic unit i.e. naphthalene containing amphiphile-**3** keeping all other structural component same as in **1**. Amphiphile-**3** showed hydrogelation ability in water at MGC =14 $mgmL^{-1}$ but at a very slow rate. It took almost 5 days to form gel in a glass vial that was stable to inversion. Generally it was found that presence of extended aromatic ring in the amphiphile's structure facilitates self-assembled gelation. Hence we introduced a pyrenyl moiety instead of naphthalene in amphiphile-**4** with an aim to improve the gelation efficiency. Amphiphile-**4** was found to gelate in water and also with improved efficiency having a MGC of 10 $mgmL^{-1}$. The decrease in MGC compared to that of **1** and **3**, (which gelate in pure water) is probably due to the additional π–π stacking interaction between pyrenyl moieties.[7a,10b] We also monitored the gelation ability of **1**-**4** in phosphate-HCl buffer of varying pH range from 3.0-7.0 (Table 1). It was found that amphiphile **1, 3** and **4** can form hydrogels at pH = 6.0 and 7.0 while amphiphile-**2** showed gelation ability only at pH = 3.0. Additionally, the amphiphile-**4** can also form hydrogel at pH = 5.0. Presumably, the tertiary nitrogen present at the terminal of the gelator motif brought the pH responsive hydrogelation behaviour through protonation at different pH.[10b] All the amphiphiles remain soluble in DMSO while amphiphile-**2** and **4** can immobilize DMSO-water solvent mixture (1:3, v/v) to form gel at MGC 10 $mgmL^{-1}$ and 10.5 $mgmL^{-1}$, respectively. Among the four amphiphiles, **4** showed better gelation efficiency in pure water and in aqueous buffer solutions possibly due

to the presence of extended aromatic ring (pyrenyl moiety) that might have facilitated the additional π–π interactions. Thus, with variation in the hydrophobic unit in the gelator's structure the gelation efficiency also modulated presumably due to the alteration in the overall HLB of the amphiphile.

On the basis of observed gelation, we have chosen hydrogelators-**1**, **3** and **4** for inclusion of various CNMs within hydrogel matrix. Gelator **2** was not considered for this study due to its inefficiency to form hydrogel in pure water as well as at pH = 7.0 phosphate-HCl buffer solution. We have selected two types of CNMs, one dimensional (1D) allotrope of carbon (Single walled pristine carbon nanotube (SWNT)) and two dimensional (2D) allotrope of carbon (graphene oxide (GO)) for their integration within hydrogel.[11] For effective inclusion of said CNMs in the gel matrix, they should be well dispersed in the aqueous medium in presence of the amphiphile. Accordingly, we first tried to disperse the amphiphobic pristine SWNT using amphiphiles-**1**, **3** and **4**.[10b] Briefly, SWNT (1 mg) was taken in 4 mL of amphiphile solution (2.5 $mgmL^{-1}$) and tip sonicated followed by bath sonication. The suspension was then centrifuged at 6000 rpm for 30 min. The supernatant was collected and the amount of dispersed SWNT was calculated using the calibration plot prepared with sodium dodecylbenzenesulfonate (SDBS).[8c] Amphiphile-**1** and -**4** showed SWNT dispersion ability of 190 μgmL^{-1} and 210 μgmL^{-1}, respectively. On the other hand, amphiphile-**3** showed moderate SWNT dispersion (55 μgmL^{-1}) probably due to its slow rate of self-assembly. Upon confirmation of the SWNT dispersion ability of **1**, **3** and **4**, amphiphiles were taken at the respective MGCs (15 $mgmL^{-1}$ for **1**, **3** and 10 $mgmL^{-1}$ for **4**) in water and sonicated after mixing with required amount of SWNT. It was then left to stand for 30 min. The formation of SWNT-gel composite was tested from the "stable to inversion" of glass vial (Figure 2). SWNT was successfully included in the hydrogel matrix of **1** and **4** to develop **1**-SWNT and **4**-SWNT nanohybrids, respectively while **3** showed poor SWNT

inclusion property due to its slow rate of gelation (Figure 2). In absence of any amphiphiles, SWNT remains insoluble in water.

We monitored the maximum inclusion amount of SWNTs within hydrogel-**1** and **4** by varying the SWNT concentration (0.25-6.0 $mgmL^{-1}$, Table 2) without compromising stability of the gel. Hydrogels-**1** and **4** maximally accommodate 3.0 and 5.0 $mgmL^{-1}$ SWNTs, respectively at their MGCs. The successful inclusion of SWNT in the entangled gel network may be attributed due to the comparable morphology and dimensions of SWNT with the gel fibres. The efficient dispersion of SWNT in aqueous solutions of amphiphile-**1** and **4** might have facilitated the successful inclusion of SWNT within the gel matrix. At this instant, we made attempt to include the 2D allotrope of carbon, i.e. GO within the SAFIN of hydrogel. Accordingly, GO was synthesized from graphite powder by a modified Hummer's method and characterized as described in the experimental section (Figure S1 in the Supporting Information).[12a] The freshly prepared GO and gelators (**1**, **3** and **4**) at their MGCs were taken in milli-Q water and probe-sonicated for 10 min at 40% power output. The resulting mixture was then allowed to cool at room temperature. Intriguingly in presence of GO, gelator-**1** lost the hydrogelation ability and GO was precipitated out from the solution (Figure 2). Similarly, amphiphile-**3** was also unable to include GO in its matrix (Figure 2). Interestingly, only hydrogel-**4** at its MGC (10 $mgmL^{-1}$ in water), formed GO included hydrogel-**4** (**4**-GO) nanocomposite. Highest inclusion ability of GO within the hydrogel-**4** was noted to be 5 $mgmL^{-1}$(Figure 2). Most likely, the pyrenyl moiety present in the gelator-**4** helped to include GO through hydrophobic and π-π interactions to form **4**-GO composite.

It is apparent from the above observations that CNM inclusion ability within hydrogel matrix is not same for all the gelators. C-16 long chain containing gelator-**1** can include only 1D allotrope of carbon (SWNT) in its SAFIN while failed to integrate 2D allotrope of carbon

(GO). Gelator-**3** was unable to integrate both SWNT and GO. Presumably, the naphthalene unit in gelator-**3** fall short to provide required hydrophobicity to facilitate its interaction with aromatic backbone of SWNT and GO. Also there could be a mismatch between the aggregated structure of **3** and CNMs. Gelator-**4** showed ability to include both 1D (SWNT) and 2D (GO) allotrope of carbon. The successful integration of SWNT and GO within the hydrogel-**4** matrix might be due to the additional π−π interaction of gelator-**4** originated from the pyrenyl group. The ultrathin honeycomb like planar structure of GO and the aromatic backbone of SWNT possibly get fitted in between the extended aromatic ring (pyrenyl moiety) through π−π stacking as well as van der Waal's interactions leading to the successful formation of **4**-GO/SWNT nanocomposite.[12b,c] Thus, modulation in the hydrophobicity in the gelator's structure led to structure dependent inclusion of different CNMs in gel matrix.

Microscopic Studies

The supramolecular morphologies of individual gels as well as SWNT/GO-integrated gels were investigated by transmission electron microscopy (TEM). The TEM images of native hydrogel-**1**, **3** and **4** in water and **2** in DMSO-water (1:3, v/v) medium showed an entangled fibrillar network with fibres of 20-50 nm in thickness (Figure 3 a-d). The helical nature of the gel fibers of hydrogel-**1** was noticed upon magnification of the TEM image (Figure S2 in the Supporting Information). Incorporation of SWNT in the hydrogel-**1** led to a change in the morphology of the **1**-SWNT composite (Figure 3e). The extent of crisscrossed intertwined network got increased in the aggregated structure of **1**-SWNT composite compared to that of native gel-**1**.[10a] In case of **4**-SWNT composite (Figure 3f), the more dense fibrillar network with thicker fibres of diameter 70-80 nm were observed than the fibres of the native hydrogel-**4**.[10b] Upon inclusion of GO in hydrogel-**4** (Figure 3g) a very thin layered structure of GO sheet interlinked with gel fibres in three dimensional (3D) network was noted.[11b] The

coexistence of intertwined fibrillar network of gelator-**4** and entrapped GO sheet was also clearly seen from the scanning electron microscopy (SEM) image of the **4**-GO composite (Figure 3h). Interestingly, the diameter of the fibres was very much comparable in both native gel and **4**-GO nanohybrid, which indicates that inclusion of GO in the gel matrix did not perturb the self-assembly of **4**.[11b] The above microscopic images of the native gel and CNMs-gel composite revealed the gelator's structure dependent successful inclusion of different CNMs within the SAFIN of hydrogels.

Determination of gel to sol transition temperature (T_{gel})

The native hydrogels and SWNT/GO-gel nanocomposites were thermo-reversible in nature and also stable at room temperature for several months. The temperature at which the gel transformed to solution is known as gel melting temperature or gel-to-sol transition temperature (T_{gel}).[10b,j] In case of hydrogel-**1**, **3** and **4** (at their MGC in water) the T_{gel} were found to be 57 °C, 61 °C and 65 °C respectively, while for hydrogel-**2** (at MGC in DMSO-water 1:3 v/v) T_{gel} was 56 °C. Interestingly, the T_{gel} of CNMs included hydrogel (at MGCs) nanohybrids were found to be higher than that of the native gel. In case of **1**-SWNT ([SWNT] = 3 mgmL^{-1}), **4**-SWNT ([SWNT] = 5 mgmL^{-1}) and **4**-GO ([GO] = 5 mgmL^{-1}), the measured T_{gel} values were 65 °C, 73 °C and 75 °C, respectively. The increment of T_{gel} values of the SWNT/GO-gel nanocomposites might be due to the enhancement in cross linking fiber between SAFIN and CNMs in the gel matrix. Consequently, higher energy/temperature was required to break the self-assembly of CNM-gels composites.

Circular dichroism (CD) study

CD spectroscopy is known to provide information about the self aggregation pattern of the small molecular mass gelators.[13] We have found different CD spectral pattern for the self-assembly of hydrogelators of **1**, **3** and **4** (Figure 4). The CD spectra of **1** (1 mgmL^{-1} in milli-Q

water) showed a negative cotton effect with double minima at 202 and 213 nm. The presence of double minima (202 and 213 nm) in the CD spectra indicates α-helicity in its self aggregation (by its pattern but not by the position of double minima).[10b,13] The helical morphology of **1** is in concurrence with the corresponding TEM image of hydrogel-**1** (Figure S2 in the Supporting Information). On the other hand, self-assembly of gelator-**3** (1 $mgmL^{-1}$ in milli-Q water) showed β–sheet (positive band at 222 nm and a negative band at 231 nm, Figure 4) pattern in its CD spectra.[13] In case of gelator-**4** (1 $mgmL^{-1}$ in milli-Q water), CD spectra showed a positive band at 226 nm and negative band at 207 nm. This type of CD spectral pattern corroborates with β-turn like self-aggregation.[13d] Hence, the hydrophobic end modulation in the gelator's structure resulted in the formation of distinctly different pattern of self-assembly for amphiphile-**1**, **3** and **4**. Presumably, these structure dependent distinctive self-aggregation patterns of the hydrogelators helped to integrate different CNMs in the gel matrix in a selective manner. Moreover, the CD spectral pattern of **1** and **4** in the presence of SWNT/GO (**1**-SWNT, **4**-SWNT and **4**-GO composites) remain unaltered with slight decrease in CD signal intensity (Figure S3 in the Supporting Information). This observation revealed the unperturbed arrangement of the supramolecular network formed by **1** and **4** upon inclusion of CNM inclusion in the hydrogel matrix.

FTIR Spectroscopy

The influence of different kinds of non-covalent interactions during the gelation process was investigated from FTIR spectra of **1** and **4** recorded in the non-aggregated state (in chloroform) as well as in gel state (in D_2O, Figure 5).[10a,b] FTIR spectra of **1** in $CHCl_3$ showed transmittance peak at approximately ν = 3292, 1643 and 1515 cm^{-1} that were originated due to $\nu_{N\text{-}H}$(amide A), amide $\nu_{C=O}$(amide I) and $\nu_{N\text{-}H}$(amide II) vibrations, respectively (Figure 5a). These peaks were shifted to approximately ν = 3377-3458 (broad

band), 1617 and 1549 cm^{-1} in D_2O. Analogous results were found in gelator-**4**, where transmittance peaks ν_{N-H} (amide A) = 3300 cm^{-1}, amide $\nu_{C=O}$ (amide I) = 1643 cm^{-1} and ν_{N-H} (amide II) = 1532 cm^{-1} were shifted ν_{N-H} (amide A) = 3352-3471 cm^{-1} (broad band), $\nu_{C=O}$(amide I) = 1609 cm^{-1} and ν_{N-H}(amide II) = 1558 cm^{-1}, respectively by changing of solvent from $CHCl_3$ to D_2O (Figure 5b). This shift in stretching and bending frequencies in D_2O indicates the involvement of intermolecular hydrogen bonding between carbonyl (C=O) and amide N-H (i.e. C=O---N-H) during the self-assembled gelation. Now it is important to know whether inclusion of SWNT/GO in the hydrogels of amphiphile-**1** and **4** affected the self-assembly of gelators. Interestingly, for xerogel of SWNT incorporated hydrogel-**1**, the amide I and amide II peaks were found to be at the similar region, 1643 and 1520 cm^{-1}, respectively (Figure S4 in the Supporting Information) to that of native gel in D_2O. In case of **4**-GO composites the peaks appeared at 1644 and 1542 cm^{-1} (Figure S4 in the Supporting Information) while **4**-SWNT showed analogous transmittance signals to that of its native hydrogel-**4**. Hence, it is evident that the integration of 1D and 2D carbon nanomaterials within the gel matrix did not perturb the intermolecular non-covalent interactions between gelators in the self-assembled state.[11]

NMR Spectroscopy

The ^{1}H-NMR study provides information about the participation of various interacting forces such as intermolecular hydrogen bonding, hydrophobic interactions etc. between the self-aggregating molecules.[10b,j] Accordingly, we performed temperature dependent (Figure 6a and b) and solvent dependent ^{1}H-NMR experiments (Figure 6c and d) for gelator **1** and **4**. Temperature dependent ^{1}H-NMR spectra of **1** (Figure 6a) in the gel state (in D_2O) at 25 °C showed that all the aromatic protons of phenyl ring are broad in nature in the region δ = 6.95-7.13 ppm. This broadening of the aromatic proton took place possibly due to the hydrophobic

interaction between the phenyl rings and the aromatic proton became more shielded. With increasing temperature, the interaction gradually reduced and more sharp and downfield shifted (δ = 7.49-7.63 ppm at 85 °C) aromatic protons were observed. Similar observation was noticed in case of **4** in D_2O (Figure 6b), where low intensity broad peak was found for the aromatic region in the gel state at 25 °C. The amide proton (N-H) of gelator-**4** appeared at δ = 7.6 ppm in the gel state and amide protons are very much shielded owing to its participation in intermolecular hydrogen bond with C=O group. The aromatic pyrenyl protons were also broadened due to efficient π–π stacking interactions. With increasing temperature, the intermolecular hydrogen bond and the π–π stacking got ruptured. As a consequence, downfield shift of aromatic and amide protons were observed at δ = 7.14-7.98 ppm and δ = 8.12-8.16 ppm, respectively with increasing sharpness in peak intensity. Interactions between aromatic rings during gelation process were further investigated from solvent dependent ^{1}H-NMR experiment. In [D_6]DMSO the aromatic proton of gelator-**1** (molecularly dissolved state) showed sharp peak at the region δ = 7.25-7.30 ppm (Figure 6c). The D_2O content of the system was gradually increased from 20 to 100%. As a result, NMR signals of the aromatic protons got broadened accompanied by the lowering in the δ value at the region of 6.96-7.14 ppm. Similar observations were found in case of gelator-**4** (Figure 6d), where upfield shift of aromatic protons was observed with widening of peaks upon increasing the D_2O content. In [D_6]DMSO the lack of non-covalent interactions makes the gelator-**1** molecules non interactive with each other for self-assembly. Upon gradual increase of D_2O content, initiation of self aggregation took place, which facilitates the π–π interaction between the phenyl ring of L-phenylalanine moiety. Similarly, in case of gelator-**4**, there is no π–π stacking between the pyrenyl moiety in [D_6]DMSO and hence characteristic aromatic proton with δ value was observed at the region δ = 7.13-7.33. With gradual increase in D_2O content an effective π–π stacking is initiated resulting in the shielding of aromatic protons

and the peak intensities notably diminished.[10b,j] The above mentioned spectroscopic and microscopic experiments delineate the participation of several non-covalent interactions in the self-assembled hydrogelation of **1** and **4**.

UV-visible spectroscopy

The aggregation pattern of small molecule gelators was also investigated from solvent dependent UV-visible study. Aggregation behaviour of molecules mainly categorized by two types i.e. *H*-type and *J*-type.[14] Molecules may self-assemble through parallel plane-to-plane stacking to form a sandwich-type array that is referred as *H*-type aggregation.[14a] Another, head-to-tail fashion arrangement (end-to-end stacking) is referred as *J*-type aggregation. In UV-vis spectra, *H*-aggregate with side-by-side alliance of molecules shows a blue-shifted absorption while *J*-aggregate with head-to-tail alignment, exhibits a red shifted absorption from its monomer units.[14] At this stage, we were keen to monitor the self aggregation type of the gelator-**1** and **4**. As the gelator-**1** was devoid of any fluorescent moiety in its structure, we have hydrophobically tagged one fluorescent probe 8-anilino-1-naphthalenesulfonic acid (ANS) in **1 (**ANS-**1)**. Hydrophobic probe ANS is supposed to interact with the hydrophobic part of the **1** and localized itself at the hydrophobic domain of the aggregate.[10j] Since gelator-**4** comprised of an intrinsically UV active pyrenyl moiety, thus no external fluorophore was needed to follow its UV-vis spectra. We have taken the UV-vis spectra of ANS-**1** ([**1**] = 0.005 mgmL^{-1}, [ANS] =1x10^{-6} M) and **4** (0.005 mgmL^{-1}) (Figure 7) in varying solvents from non-gelating (DMSO) to a gelating one (water). ANS-**1** showed a broad band at 367 nm in DMSO which red shifted to 380 nm upon changing the solvent to milli-Q water (Figure 7a). This red shift clearly indicates the *J*-type aggregation pattern of **1** (Figure 8).[14b,c] Presumably, this distinct *J*-type self-assembly of gelator-**1** assisted spiral coiling in the gel fibers as observed from the TEM image (Figure S2 in the Supporting Information). Interestingly, gelator-**4** (0.005 mgmL^{-1}) in non-gelating solvent (in DMSO), showed a sharp

band of pyrene at 328 and 345 nm due to π–π* transitions (Figure 7b). Changing the solvent system from DMSO to water, the π–π* transition bands blue shifted to 325 and 340 nm, respectively. It suggested that the self assembly took place through *H*-type aggregation pattern i.e. sandwich type parallel layer formation (Figure 8).[14a] This distinctive parallel layer by layer orientation of hydrogelator-**4** probably helped in successful GO inclusion in hydrogel-**4** matrix compared to other hydrogels. Subsequently, it may be inferred that *J*-type aggregation helped to integrate only 1D allotrope of carbon and *H*-type self-aggregation would be suited well for incorporation of both 1D and 2D allotrope of carbon (Figure 8).

Fluorescence study

Hydrophobic interaction is a much-discussed phenomenon in self-assembled hydrogelation. To this end, we carried out the fluorescence spectroscopic study using 8-anilino-1-naphthalenesulfonic acid (ANS) during hydrogelation of **1** (Figure 9a). ANS has emission maxima (λ_{max}) at 509 nm in water upon excitation at 365 nm. The fluorescence intensity of ANS increased in presence of **1** and it gradually enhanced as the concentration of **1** was increased from 0.015 to 0.6 mgmL^{-1}). The increase in fluorescence intensity was accompanied by a blue shift from 509 nm to 479 nm (Figure 9a). Notably, the λ_{max} of ANS intensity got decreased with a blue-shift at 470 nm when the gelator concentration was further increased to 1.5 mg mL^{-1}. The above results indicated that upon self-assembly of **1**, ANS started to experience hydrophobic environment. However the fluorescent probe experienced less hydrophobic environment in the gel state compared to that of the intermediate state of gelation.[10j,15] Thus, gelation process seemed to undergo via an intermediate state of self-assembly to which ANS had a superior binding affinity compared to the gel state. In case of the gelator-**4**, at concentration of 0.01 mgmL^{-1} (~1000 times lower than MGC), strong emission maxima was found at 397 nm along with other peaks at 378 nm and 419 nm upon

excitation at 340 nm (Figure 9b). At this concentration, the molecule is evidently in non-self-assembled state in accordance to the characteristics emission spectrum of **4**. Upon increasing the gelator concentration to 0.1 mg mL^{-1}, formation of a new excimer peak was noted at a higher wavelength (λ = 469 nm) possibly due to the interactions between the pyrene moieties in the self assembled state through π–π interactions.[10b,11b] Also the bathochromic shift in fluorescence emission maxima is due to the strong intermolecular hydrogen bonding between the LMWG molecules. Furthermore, we have taken the fluorescence spectra of CNM included hydrogel-**4** (0.5 $mgmL^{-1}$) keeping SWNT and GO concentrations fixed at 0.5 $mgmL^{-1}$ and 0.075 $mgmL^{-1}$, respectively (Figure 9c). Quenching of fluorescence intensity was evident from the emission spectra of both SWNT and GO included gel nano-hybrid compared to that of native hydrogel. The reduced intensity in fluorescence spectra of **4**-SWNT and **4**-GO hybrid confirmed the successful integration of nanotubes and nanosheets within the SAFIN of the gel. The possible interaction between hydrophobic pyrene moiety and aromatic backbone of both SWNT /GO resulted in the quenching of fluorescence intensity.[10b,11b] Moreover the decrease in fluorescence emission intensity can also be noticed visually. A bright blue light emission of native hydrogel-**4** upon UV irradiation (365 nm) got significantly reduced by inclusion of SWNT/GO in the gel matrix (Figure 9d).

Steady state fluorescence anisotropy

Steady state fluorescence anisotropy is an excellent tool for measuring the fluidity of a system using a fluorescence probe. The most common probe used to measure fluorescence anisotropy is 1,6-diphenyl-1,3,5-hexatriene (DPH), which intercalates between the hydrophobic interior of the aggregates due to its rod-like shape and hydrophobic nature.[16a] The higher steady state anisotropy (*r*) value indicates the restricted movement of DPH in varying aggregated structure.[16b-c] We have used this technique to understand the gelation

mechanism of **1**. It is observed that at a low concentration of **1** (0.20 mgmL^{-1}) in water, DPH showed relatively large *r* value (0.13, Table 3). At a lower concentration of amphiphile (below or around the critical micellar concentration, cmc), DPH molecules aggregate with each other showing a higher anisotropy.[10j,16d] However, *r* value remain unaltered (*r* = 0.10, Table-3) with increasing concentration of **1** (0.30-3.0 mg mL^{-1}, Table 3). Presumably above cmc, DPH molecules become solubilized in the hydrophobic interior of the micelles with lower microviscosity.[10j] Notably, in case of a micellar solution of common surfactant, cetyltrimethylammonium chloride (CTAC) within the concentration range of 5-100 mM, the *r* value was found to be 0.06. The higher anisotropy for **1** (*r* = 0.10) compared to that for CTAC (*r* = 0.06) indicates that the aqueous solution of **1** is a more viscoelastic system. The microviscosity of the **1** solution is higher probably because of the formation of elongated micelles (rod or worm-like).[10j] So on the basis of above observation, it may be inferred that the formation of hydrogel of **1** (MGC = 15 mgmL^{-1}) is processed by changing the topology from elongated micelles to fibrillar network upon increase in the concentration of **1**. We have failed to perform fluorescence anisotropy experiment with gelator-**4** as it contains intrinsically fluorescent pyrene unit, which interferes in the anisotropy experiment as the excitation wavelength of pyrene is almost comparable with DPH (λ_{ex}=370 nm).

Rheology

At this instant, it would be fascinating to find out how the stiffness of the gel changed upon addition of CNM in to the gel matrix. Rheological studies provide information on the fluidity and rigidity of viscoelastic materials such as gels.[10a] Two major parameters related to the viscoelasticity are the storage modulus (*G′*) and the loss modulus (*G″*). The storage modulus *G′* stands for the ability of a deformed material to restore its native form whereas the loss modulus *G″* represents the flow behavior of the material under applied stress.[10a,b] For

viscoelastic materials like gels $G' > G''$ (G' and $G'' = \omega^0$, ω=angular frequency), and in the sol state $G'' > G'$ ($G' = \omega^2$ and $G'' = \omega$). Initially we studied the mechanical stiffness of native hydrogels-**1** and **4** at their respective MGCs (15 and 10 $mgmL^{-1}$, respectively) by an oscillatory frequency sweep experiment in which G' and G'' were recorded as a function of angular frequency (in the range 0.1–600 rad s^{-1}) at a fixed strain of 0.01% (Figure 10). Native hydrogel-**1** and **4** exhibited G' values of 410 and 585 Pa, respectively. Interestingly, upon inclusion of pristine SWNTs into hydrogel-**1**, the value of G' increased by ~2 fold (G'=805 Pa) compared to the native gel at SWNT concentration = 1.5 $mgmL^{-1}$. On the other hand, the GO (1.5 $mgmL^{-1}$) included hydrogel-**4** showed merely 1.06 fold improvement in G' value (G'=622 Pa). However, **4**-GO with 3 $mgmL^{-1}$ GO content showed ~1.7 fold (G'=988 Pa) enhanced mechanical rigidity than that of the native hydrogel. The above results delineate that the enhanced cross-linking between the SWNT/GO and the SAFIN led to better mechanical resistance of the soft nanocomposites.

Conclusions

In brief, suitable hydrophobic residue tailored L-phenylalanine containing triethylene glycol monomethyl ether attached neutral hydrogelators were synthesized. These gelators self-assembled to form hydrogel in water and aqueous buffer solutions (pH ranging from 3-7). The critical role of HLB in self-assembled gelation was analysed by altering the hydrophobic residue from long chain C-16 to extended aromatic pyrenyl group. Moreover, the involvement of various interactions in gelation and gelator structure dependent inclusion of 1D and 2D allotrope of carbon nanomaterials within the SAFIN was investigated from spectroscopic and microscopic studies. Interestingly, C-16 long chain containing gelator-**1** can successfully include 1D allotrope of carbon (SWNT) while pyrene containing gelator-**4** include both 1D and 2D allotrope of carbon (SWNT and GO, respectively). *J*-type and *H*-

type self-aggregation pattern of the hydrogelator-**1** and **4**, respectively might have facilitated the structure dependent inclusion of CNMs within hydrogel. Hence, the modulation in the hydrophobic terminal of gelators has notable influence in its self-aggregation as well as integration of CNMs of different dimension. Moreover, rheological studies of the hydrogel and SWNT/GO-gel composite delineate that the inclusion of SWNT/GO within the hydrogels improved the mechanical stiffness of the resulting soft-nanocomposites than that of the native hydrogels.

Experimental section

Materials:

L-phenylalanine, naphthalene-1-acetic acid, dicyclohexylcarbodiimide (DCC), 4-*N*,*N*-(dimethyl)aminopyridine (DMAP), 1-hydroxybenzotriazole (HOBT), Di-tert-Butyldicarbonate (BOC anhydride), silica gel 60-120 and 100-200 mesh, solvents were purchased from SRL, India. Trifluoroacetic acid (TFA) and sodium hydroxide pellets, potassium carbonate, thionyl chloride were brought from Spectrochem, India. Palmitic acid, pyrene butyric acid, 2,2′-(ethylenedioxy) bis (ethylamine), triethylene glycol monomethyl ether (TEG), tosyl chloride, single walled carbon nanotube (SWNT), graphite powder, $CDCl_3$, [D_6]DMSO and D_2O were procured from Sigma. All deuteriated solvents for NMR and FTIR experiments were obtained from Aldrich Chemical Co. Thin-layer chromatography was performed on Merck pre-coated silica gel 60-F_{254} plate. Lyophilization was done in a Virtis 4KBTXL-75 freeze-drier. Mass spectrometric data were acquired by the electron spray ionization (ESI) technique on a Q-tof-micro quadrupole mass spectrometer (Micromass). ^{1}H NMR spectra were recorded by using an AVANCE 500 MHz (Bruker) spectrometer. Elemental analyses were performed by using a Perkin–Elmer 2400 CHN analyzer. High resolution transmission electron microscopy (TEM) images were taken on a JEOL JEM 2010 high-resolution microscope operating at 200 kV. Field emission scanning electron

microscopy (SEM) study was done on a JEOL-6700F microscope. The UV-vis absorption spectra were recorded on a PerkinElmer Lambda 25 spectrophotometer. Fluorescence spectra were recorded in Varian Cary Eclipse luminescence spectrometer. FTIR spectra were recorded in a Perkin Elmer Spectrum 100 spectrometer. XRD measurements were done with a Seifert XRD 3000P diffractometer and the source was a Cu Kα radiation (α =0.15406 nm) with a voltage and current of 40 kV and 30 mA. Probe sonication and bath sonication was performed using an Omni Sonic Ruptor 250 and Telsonic Ultrasonic bath sonicator, respectively.

Synthesis of amphiphilic gelator 1-4:

All the amphiphiles were synthesized by following very well established peptide chemistry (Scheme S1 and S2 in the Supporting Information). The carboxylic acid group of the L-phenylalanine was converted to a methyl ester. The ester-protected amino acid was coupled with palmitic acid with DCC (1 equiv), DMAP (cat.), and HOBt (1 equiv) in dry DCM (CH_2Cl_2). The ester protected amide was purified by column chromatography on 60-120 mesh silica gel (methanol/chloroform). The product was then hydrolyzed by treating with 1N NaOH solution (1.1 equiv) in MeOH for 6 h with stirring at room temperature. The reaction mixture was concentrated on a rotary evaporator and then diluted with water. The aqueous mixture was washed with diethyl ether and subsequently acidified with a 1N aqueous HCl solution and the produced carboxylic acid was extracted with ethyl acetate. This acid was coupled with mono-Boc-protected 2,2'-(ethylenedioxy)bis(ethylamine) by treating with DCC (1 equiv), DMAP (cat.), and HOBT (1 equiv) in dry CH_2Cl_2. The product was purified by column chromatography on 100–200 mesh silica gel (methanol/chloroform). Purified product was subjected to deprotection of Boc for 3 h stirring with trifluoroacetic acid (TFA) (4 equivalent) in dry DCM. Solvent was removed on a rotary evaporator and the mixture was

taken in ethyl acetate (EtOAc). The EtOAc part was thoroughly washed with 10% aqueous sodium carbonate (Na_2CO_3) solution followed by brine to neutrality. The organic part was dried over anhydrous sodium sulfate and concentrated to get the corresponding amine. The product was purified by column chromatography on 100–200 mesh silica gel (methanol/chloroform as eluent). In the final step, to obtain the hydrophilic triethylene glycol monomethyl ether (TEG) substituted product, the pure amine was subjected to nucleophilic substitution under refluxing condition in dry acetonitrile (CH_3CN) in presence of anhydrous K_2CO_3 (2.5 equiv) at 70 °C. Accordingly, the reaction mixture was filtered and the desired product (**1**) was purified by column chromatography on 100-200 mesh silica gel (methanol/chloroform). Similar protocol was applied to synthesize **2-4** using C-16 chain protected L-phenylalanine, naphthalene-1-acetic acid and 1-pyrenebutyric acid (Scheme S1 and S2 in the Supporting Information).^{1}H-NMR spectroscopic and mass spectroscopic analysis of **1**, **2**, **3** and **4** are provided in the Supporting Information.

Preparation of hydrogels:

The requisite amount of **1**, **3** and **4** were taken in screw capped vial having internal diameter (i.d.) of 10 mm and slowly heated to dissolve in Milli-Q water and in various phosphate-HCl buffer solution (pH = 3.0-7.0). The gelation ability of **2** was tested in DMSO-H_2O (1:3, v/v). The solution was allowed to cool slowly (undisturbed) to room temperature. The gelation was checked by "stable to inversion" of the aggregated material in the glass vial.

Determination of gel-to-sol transition temperature (T_{gel}):

The gel-to-sol transition temperature (T_{gel}) was recorded by gradually increasing the temperature (at a rate of 2 °C min^{-1}) in the thermostatted oil bath in which the hydrogel containing glass vial (i.d. 10 mm) was placed. The temperature (±0.5 °C) at which the gel liquified and started to flow under gravitation is referred as T_{gel}.

Synthesis of graphene oxide (GO):

Graphene oxide (GO) was synthesized from graphite powder (<30 mm) following the modified Hummer's method. Graphite powder (0.5 g) was dispersed in 20 mL concentrated H_2SO_4 and then sodium nitrate (0.5 g) was added to the dispersion and it was cooled to 0 °C. Then $KMnO_4$ (1.5 g) was slowly added to the mixture so that the temperature always remains <20 °C and mixed thoroughly. The resulting solution was transferred to 35 °C water bath and stirred for 30 min. The temperature was raised to 90 °C during the addition of 30 mL of water and it was maintained for another 15 min. The whole solution was then mixed in 80 mL of warm water. To this solution, 0.5 mL 30% H_2O_2 was added to reduce the residual permanganate. The solution was filtered and washed thoroughly with warm water. The solid was dispersed in 100 mL distilled water by sonication. This dispersion was centrifuged at 3000 rpm for 15 min. The residue was suspended in water by sonication and again centrifuged at 20000 rpm. This suspension/centrifugation process was repeated for 2 times. Finally the semi-solid residue was collected and freeze dried in vacuum to obtain GO. The formation of GO was further characterized by UV-vis spectroscopy and X-ray diffraction study (XRD).

Preparation of SWNT/GO included gel nanocomposites:

Required amount of SWNT was weighed in the screw capped glass vial with internal diameter of 10 mm. An aqueous solution (1 mL) of both amphiphiles (**1** and **4**) having the required concentration was added and tip sonicated for 10 min at 30% power output. The solutions were then left undisturbed for 30 min to form a nanohybrid gel (**1**-SWNT and **4**-SWNT) that was stable to the inversion of the glass vial. Similar protocol was performed in case of preparation of GO included nanocomposite (**4**-GO). The required amount of GO was weighed and an aqueous solution of amphiphile-**4** (1 mL) with desired concentration was added and again tip sonicated for 10 min at 40% power output. The solution was kept

carefully at room temperature for half an hour to prepare the soft-nanocomposite (**4**-GO) having restricted mobility of solvent.

Microscopic study:

Field-emission scanning electron microscopy (SEM) images were obtained on a JEOL-6700F microscope. A drop of gel (at the MGC) was placed on a piece of cover slip and dried for a few hours under vacuum before imaging. TEM experiments were performed on a JEOL JEM 2010 high-resolution microscope operated at an accelerating voltage of 200 kV. A dilute solution of gel was placed on a 300 mesh carbon-coated Cu grid and dried for a few hours under vacuum before imaging.

Circular dichroism:

CD spectra of an aqueous solution of gelator-**1**, **3** and **4** at varying concentrations were recorded by using a quartz cuvette of 1 mm path length in a JASCO J-815 CD spectropolarimeter.

FTIR measurements:

FTIR measurements were performed with gelators in non-self-assembled state in $CHCl_3$, in the gel state in D_2O and in dried condition for the hydrogel-**1** and **4** as well as for SWNT/GO nanocomposites (**1**-SWNT, **4**-SWNT and **4**-GO) at room temperature. All the experiments were carried out in a Perkin–Elmer Spectrum 100 FTIR spectrometer using KBr pellets (for $CHCl_3$ solutions and xerogels) and a 1 mm CaF_2 cell (for D_2O gels).

Temperature and solvent dependent ^{1}H NMR measurements:

Temperature dependent ^{1}H NMR spectra of **1** and **4** were recorded on an Avance 300 MHz (Bruker) spectrometer at a concentration of 15 $mgmL^{-1}$ and 10 $mgmL^{-1}$, respectively in D_2O at varying temperature (25-85 °C). Solvent dependent ^{1}H NMR spectra of **1** and **4** were also recorded on at MGC for both **1** and **4** at varying solvent ratio of D_2O and [D_6]DMSO.

UV-Vis spectroscopy:

The UV-Vis spectra of ANS doped gelator-**1** and native gelator-**4** were recorded on a PerkinElmer Lambda 25 spectrophotometer by varying the solvent from non-gelating (DMSO) to gelating one (Milli-Q water).

Fluorescence spectroscopy:

The emission spectra of ANS and aqueous solutions of ANS doped hydrogel-**1** were recorded in a Varian Cary Eclipse luminescence spectrometer. The probe molecules were added to the aqueous solutions of amphiphiles at varying concentrations at room temperature. ANS stock solution was prepared in MeOH and from this super stock solution the required amount of ANS solutions were added to gelators so that the final concentration of ANS solution was $1x10^{-5}$ M. The ANS solution was excited at 360 nm (λ_{ex}). Fluorescence study of the gelator-**4** was carried out by recording the spectra of amphiphilic solution excited at 340 nm (λ_{ex}) at varying concentration of the gelator. The excitation and emission slit width were both 5 nm.

Steady state fluorescence anisotropy study:

Steady-state fluorescence anisotropic study was performed using fluorescent probe DPH in aqueous solution of surfactant in a Varian Cary Eclipse luminescence spectrometer. Stock solution of DPH was prepared in tetrahydrofuran (THF), keeping the final concentration 2 x 10^{-6} M for DPH. The aqueous solutions were excited at 370 nm for DPH and the corresponding emission spectra were recorded at 450 nm. The excitation and emission slit width were 2.5 nm and 5 nm. The fluorescence anisotropic value (r) was calculated by the instrumental software using the equation

$$r = (I_{VV}-GI_{VH}) / (I_{VV}+2GI_{VH})$$

where I_{VV} and I_{VH} are, respectively, the fluorescence intensities of the emitted light polarized parallel and perpendicular to the excited light and $G = I_{VV}/I_{VH}$ is the instrumental grating factor. The fluorescence measurements were performed at 25 °C.

Rheology:

Rheological experiments were carried out in cone and plate geometry (diameter 40 mm) on the rheometer plate using an Anton Paar MCR 302 instrument. The native gels (**1** and **4**) and the SWNT–gel (**1**-SWNT) and GO-gel (**4**-GO) composites were scooped on the rheometer plate so that there was no air gap with the cone. Frequency sweep experiments were performed as a function of angular frequency (0.1–200 rad s^{-1}) at a fixed strain of 0.01% at 25 °C and the storage modulus (G') and the loss modulus (G'') were plotted against angular frequency (ω).

Acknowledgements:

PKD is thankful to Department of Science and Technology, India (SR/S1/OC-25/2011) for financial assistance. PC, DM and SB acknowledge Council of Scientific and Industrial Research, India for Research Fellowships.

Supporting information available: Synthetic scheme of **1**-**4**, characterization of gelator **1**-**4** (^{1}H-NMR, Mass spectrometry, CHN data), UV-vis absorbance spectra of GO and XRD spectra of GO, TEM image of the dried hydrogel-**1**, FTIR spectra of xerogel of **1**, **4**, **1**-SWNT, **4**-SWNT and **4**-GO. Supporting information for this article is available on the website under http://www.chemeurj.org/ or from the author.

References:

[1] a) D. Ma, K. Tu, L. M. Zhang, *Biomacromolecules* **2010**, *11*, 2204; b) D. M. Ryan, B. L. Nilsson, *Polym. Chem.* **2012**, *3*, 18.

[2] a) M. J. Wilson, S. J. Liliensiek, C. J. Murphy, W. L. Murphy, P. F. Nealey, *Soft Matter* **2012**, *8*, 390; b) D. Kalafatovic, M. Nobis, N. Javid, P. W. J. M. Frederix, K. I. Anderson, B. R. Saunders, R. V. Ulijn, *Biomater. Sci.* **2015**, *3*, 246.

[3] a) E. Caló, V. V. Khutoryanskiy, *European Polymer Journal* **2015**, *65*, 252; b) J. Wan, *Analytica Chimica Acta.* **1999**, *399*, 21.

[4] a) C. C. Beozzo, M. A. Alves-Rosa, S. H. Pulcinelli, C. V. Santilli, *Materials* **2013**, *6*, 1967; b) R. Kumar, K. Jayaramulu, T. K. Maji, C. N. R. Rao, *Dalton Trans. (Communication)* **2014**, *43*, 7383; c) A. Chakrabarty, U. Maitra, *J. Phys. Chem. B* **2013**, *117*, 8039; d) P. K. Vemula, G. John, *Chem. Commun.* **2006**, 2218.

[5] a) S. K. Samanta, S. Bhattacharya, *J. Mater. Chem*., **2012**, *22*, 25277; b) Y. M. Abul-Haija, R. V. Ulijn, *Biomacromolecules* **2015**, *16*, 3473; d) J. M Poolman, J. Boekhoven, A. Besselink, A. G L Olive, J. H van Esch, R. Eelkema, *Nat. Protoc.* **2014**, *9*, 977; e) B. Escuder, F. Rodríguez-Llansola, J. F. Miravet, *New. J. Chem.* **2010**, *34*, 1044; f) J. D. Decoppet, T. Moehl, S. S. Babkair, R. A. Alzubaydi, A. A. Ansari, S. S. Habib, S. M. Zakeeruddin, H. W Schmidt, M. Grätzel, *J. Mater. Chem. A* **2014**, *2*, 15972.

[6] a) D. Das, T. Kar, P. K. Das, *Soft Matter* **2012**, *8*, 2348; b) S. Srinivasan, V. K. Praveen, R. Philip, A. Ajayaghosh, *Angew. Chem.* **2008**, *120*, 5759; *Angew. Chem. Int. Ed.* **2008**, *47*, 5675; c) A. T. Haedler, K. Kreger, A. Issac, B. Wittmann, M. Kivala, N. Hammer, J. Köhler, H. W. Schmidt, R. Hildner, *Nature* **2015**, *523*, 196; d) I. Sittko, K. Kremser, M. Roth, S. Kuehne, S. Stuhr, J. C. Tiller, *Polymer* **2015**, *64*, 122; e) S. Bhattacharjee, S. K. Samanta, P. Moitra, K. Pramoda, R. Kumar, S. Bhattacharya, C. N. R. Rao, *Chem. Eur. J.* **2015**, *21*, 5467; f) C. Krumm, S. Harmuth, M. Hijazi, B. Neugebauer, A. L. Kampmann, H. Geltenpoth, A. Sickmann, J. C. Tiller, *Angew. Chem.* **2014**, *126*, 3908; *Angew. Chem. Int. Ed.* **2014**, *53*, 3830; g) J. Gao, H. Wang, L. Wang, J. Wang, D. Kong, Z. Yang, *J. Am. Chem. Soc.* **2009**, *131*, 11286.

[7] a) D. Mandal, S. K. Mandal, P. K. Das, *Chem. Eur. J.* **2015**, *21*, 12042; b) B. Xing, C. W. Yu, K. H. Chow, P. L. Ho, D. Fu, B. Xu, *J. Am. Chem. Soc.* **2002**, *124*, 14846; c) H. Kobayashi, A. Friggeri, K. Koumoto, M. Amaike, S. Shinkai, D. N. Reinhoudt, *Org. Lett.* **2002**, *4*, 1423; d) L. A. Estroff, A. D. Hamilton, *Angew. Chem.* **2000**, *112*, 19; *Angew. Chem. Int. Ed.*, **2000**, *39*, 3447.

[8] a) A. S. Hoffman, *Advanced Drug Delivery Reviews* **2012**, *64*, 18; b) J. Bergera, M. Reista, J. M. Mayera, O. Feltb, N. A. Peppasc, R. Gurny, *European Journal of Pharmaceutics and Biopharmaceutics* **2004**, *57*, 19 ; c) S. Brahmachari, D. Das, P. K. Das, *Chem. Commun.* **2010**, *46*, 8386; d) F. Zhao, M. L. Ma, B. Xu, *Chem. Soc. Rev.*, **2009**, *38*, 883; e) G. Liang, Z. Yang, R. Zhang, L. Li, Y. Fan, Y. Kuang,Y. Gao, T. Wang, W. W. Lu, B. Xu, *Langmuir* **2009**, *25*, 8419; f) Y. Tian, H. Wang, Y. Liu, L. Mao, W. Chen, Z. Zhu, W. Liu,W. Zheng, Y. Zhao, D. Kong, Z. Yang, W. Zhang, Y. Shao, X. Jiang, *Nano Lett.* **2014**, *14*, 1439.

[9] a) S. S. Babu, V. K. Praveen, A. Ajayaghosh, *Chem. Rev*. **2014**, *114*, 1973; b) K. Naoi, S. Ishimoto, J. Miyamotoad, W. Naoi, *Energy Environ. Sci.* **2012**, *5*, 9363; c) G. Vilaca, B. Jousseaume, C. Mahieux, C. Belin, H. Cachet, M. C. Bernard, V. Vivier, T. Toupance, *Adv. Mater*. **2006**, *18*, 1073; d) H. Li, J. Choi, T. Nakanishi, *Langmuir* **2013**, *29*, 5394; e) D. Depan, A. P. Kumar, R. P. Singh, *Acta Biomaterialia* **2009**, *5*, 93.

[10] a) S. K. Mandal, T. Kar, D. Das, P. K. Das, *Chem. Commun*., **2012**, *48*, 8389; b) D. Mandal, T. Kar, P. K. Das, *Chem. Eur. J.* **2014**, *20*, 1349; c) R. Liu, S. M. Mahurin, C. Li, R. R. Unocic, J. C. Idrobo, H. Gao, S. J. Pennycook, S. Dai, *Angew. Chem.* **2011**, *123*, 6931; *Angew. Chem. Int. Ed.* **2011**, *50*, 6799; d) M. Tunckol, J. Durand, P. Serp, *Carbon* **2012**, *50*, 4303 ; e) Yang, G. Zhang, D. Zhang, J. Xiang, G. Yang, D. Zhu, *Soft Matter* **2011**, *7*, 3592; f) J. Liu, G. Chen, M. Jiang, *Macromolecules* **2011**, *44*, 7682; g) M. J. Allen, V. C. Tung, R. B. Kaner, *Chem. Rev.* **2010**, *110*, 132; h) J. I. Paredes, S. Villar-Rodil, A. Martínez-Alonso, J. M. D. Tascón, *Langmuir* **2008**, *24*, 10560; i) O. C. Compton, S. T. Nguyen, *Small* **2010**, *6*, 711; j) S. Dutta, A. Shome, S. Debnath, P. K. Das, *Soft Matter* **2009**, *5*, 1607.

[11] a) C. Maity, W. E. Hendriksen, J. H. van Esch, R. Eelkema, *Angew. Chem.* **2015**, *127*, 1012; *Angew. Chem. Int Ed.* **2015**, *54*, 998, b) S. K. Mandal, D. Mandal, P. K. Das,

ChemPlusChem **2015**, DOI: 10.1002/cplu.201500457; c) S. K. Samanta, K. S. Subrahmanyam, S. Bhattacharya, C. N. R. Rao, *Chem. Eur. J.* **2012**, *18*, 2890; d) J. Wu, A. Chen, M. Qin, R. Huang, G. Zhang, B. Xue, J. Wei, Y. Li, Y. Cao, W. Wang, *Nanoscale*, **2015**, *7*, 1655.

[12] a) W. S. Hummers, R. E. Offeman, *J. Am. Chem. Soc*. **1958**, *80*, 1339; b) M. Yoshida, N. Koumura, Y. Misawa, N. Tamaoki, H. Matsumoto, H. Kawanami, S. Kazaoui, N. Minami, *J. Am. Chem. Soc.* **2007**, *129*, 11039; c) J. Liu, G. Chen, M. Jiang, *Macromolecules* **2011**, *44*, 7682; f) M. J. Allen, V. C. Tung, R. B. Kaner, *Chem. Rev.* **2010**, *110*, 132.

[13] a) B. Escuder, J. F. Miravet, *Langmuir* **2006**, *22*, 7793; b) I. Laczko, E. Vass, K. Soos, L. Fulop, M. Zarandi, B. Penke, *J. Pept. Sci.* **2008**, *14*, 731; c) N. J. Greenfield, *Nat Protoc*. **2006**, *1*, 2876; d) C. A. Bush, S. K. Sarkar, K. D. Kopple, *Biochemistry* **1978**, *17*, 4951.

[14] a) Y. Dong, B. Xu, J. Zhang, X. Tan, L. Wang, J. Chen, H. Lv, S. Wen, B. Li, L. Ye, B. Zou, W. Tian, *Angew. Chem.* **2012**, *124*, 10940; *Angew. Chem. Int. Ed*. **2012**, *51*, 10782; b) Y. Hirano, Y. Tokuoka, N. Kawashima, Y. Ozaki, *Vib. Spectrosc.*, **2007**, *43*, 86; c) A. D'Urso, M. E. Fragala, R. Purrello, *Chem. Commun*. **2012**, *48*, 8165.

[15] U. Maitra, S. Mukhopadhyay, A. Sarkar, P. Rao, S. S. Indi, *Angew. Chem.* **2001**, *113*, 2341; *Angew. Chem. Int. Ed.* **2001**, *40*, 2281.

[16] a) A. J. C. Fulford, W. E. Peel, *Biochim. Biophys. Acta* **1980**, *598*, 237; b) S. Bhattacharya, Y. K. Ghosh, *Langmuir* **2001**, *17*, 2067; c) S. Mukhopadhay, I. G. Krishnamoorthy, U. Maitra, *J. Phys. Chem. B* **2003**, *107*, 2189

Table 1 Minimum gelation concentration (MGC) of **1-4** in different aqueous medium.

Solvents	**1** ($mgmL^{-1}$)	**2** ($mgmL^{-1}$)	**3** ($mgmL^{-1}$)	**4** ($mgmL^{-1}$)
Milli-Q water	15.0	Ins	14.0	10.0
pH=7	15.3	Ins	11	11.0
pH=6	15.1	Ins	11	9.4
pH=5	Sol	Ins	Sol	8.8
pH=3	Sol	12.0	Sol	Sol
DMSO-water (1:3, v/v)	Sol	10.0	Sol	10.5

[Sol= Soluble, Ins= Insoluble]

Table 2 Maximum accommodation of pristine SWNT and GO in hydrogels of **1** and **4** at their MGCs at 25 °C.

Gelator	[SWNT] in hydrogel ($mgmL^{-1}$)	[GO] in hydrogel ($mgmL^{-1}$)
1	3.0	-
4	5.0	5.0

Table 3 Steady-state fluorescence anisotropic (*r*) values of DPH for gelator-**1** in water

Concentration ($mgmL^{-1}$) of gelator-**1**	*r*
0.20	0.13
0.30	0.10
0.60	0.10
1.50	0.10
3.00	0.10

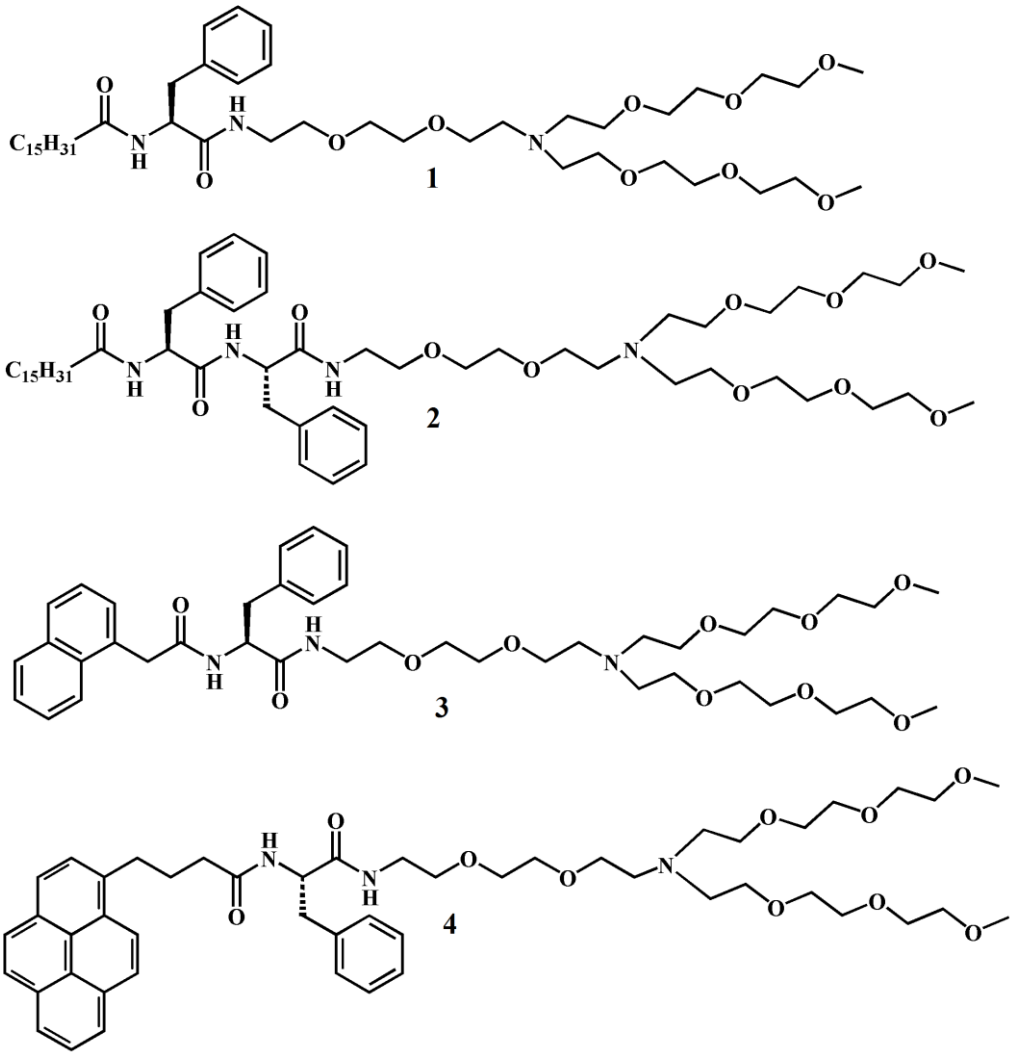

Figure 1. Structures of the amphiphilic gelators **1-4**.

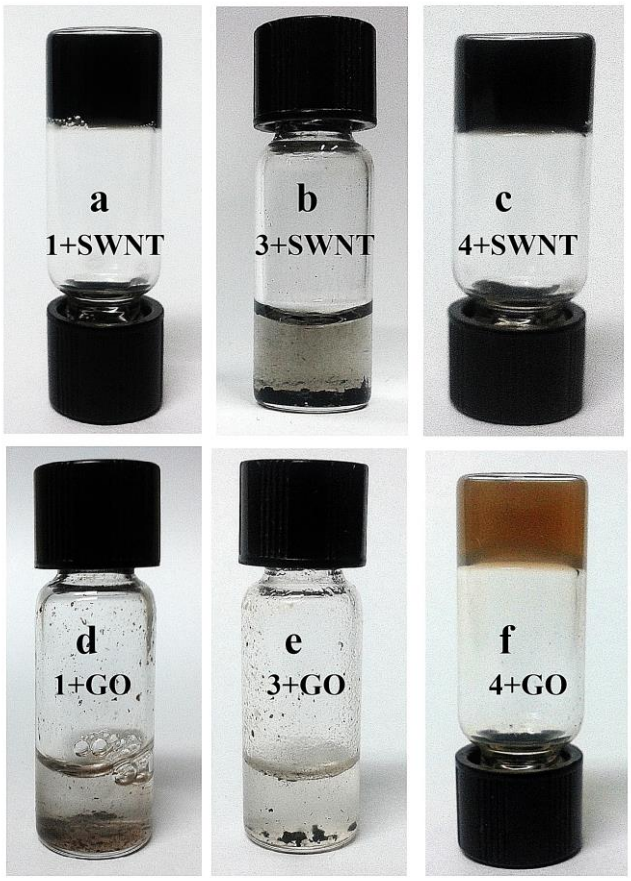

Figure 2. Inclusion and precipitation of SWNT and GO in hydrogels of **1**, **3** and **4**.

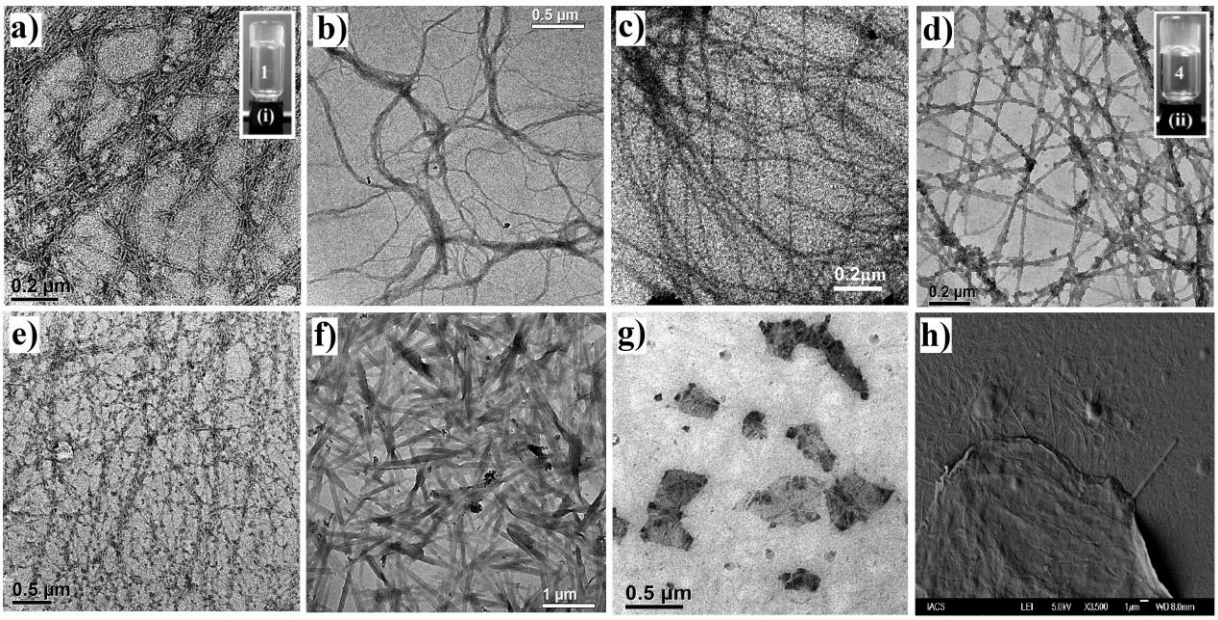

Figure 3. TEM images of hydrogel **1**-**4** (a-d, respectively). Inset of a and d showed the photographic images of hydrogel-**1** and **4**, respectively. TEM images of (e) **1**-SWNT, (f) **4**-SWNT and (g) **4**-GO composite. (h) SEM image of **4**-GO.

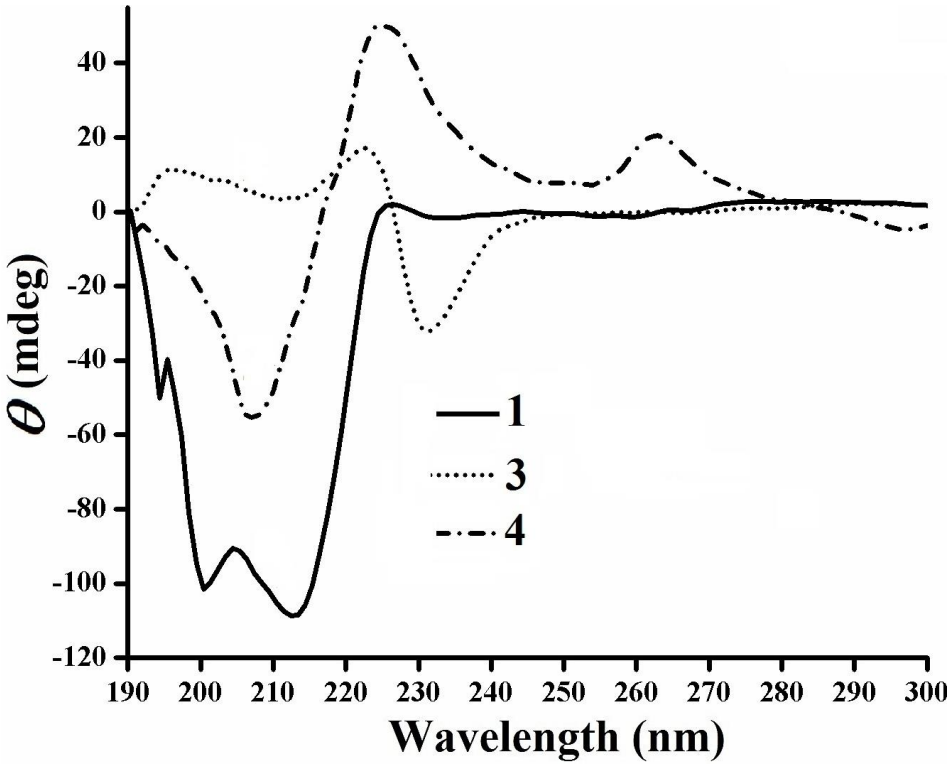

Figure 4. CD spectra of amphiphilic gelators **1**, **3** and **4**.

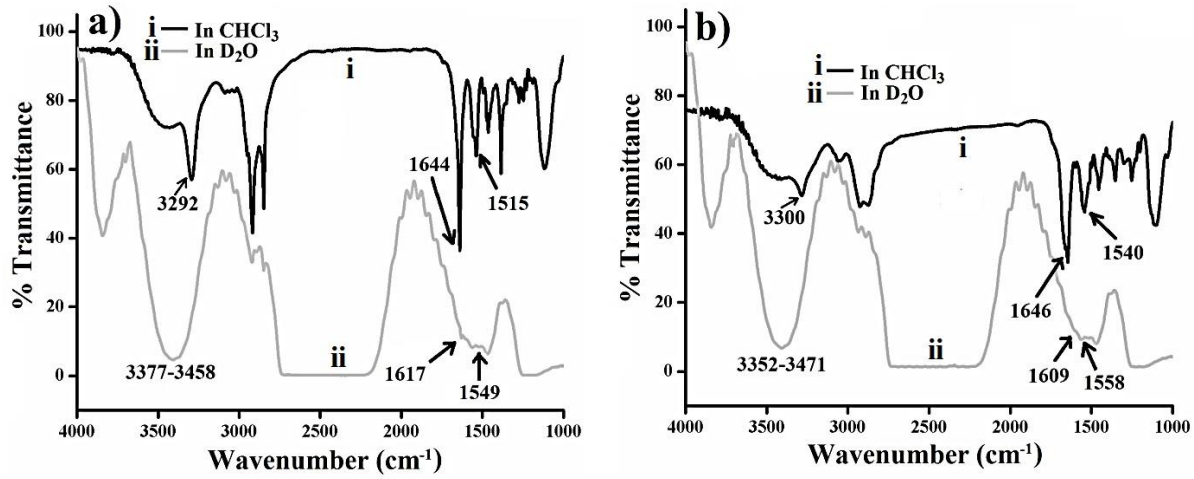

Figure 5. FTIR spectra of (a) **1** and (b) **4** in the respective solvents.

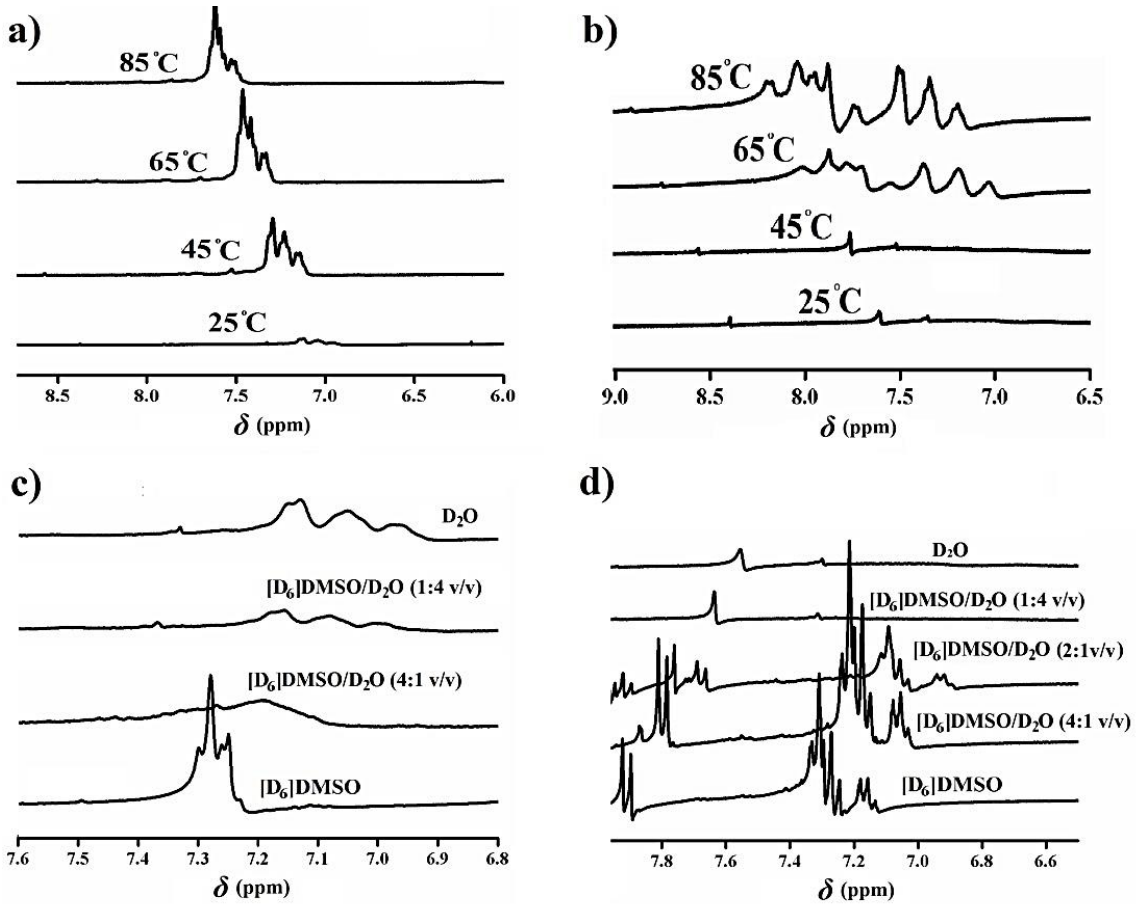

Figure 6. Temperature dependent ^{1}H-NMR spectra of (a) **1** and (b) **4**. Solvent dependent ^{1}H-NMR spectra of (c) **1** and (d) **4**.

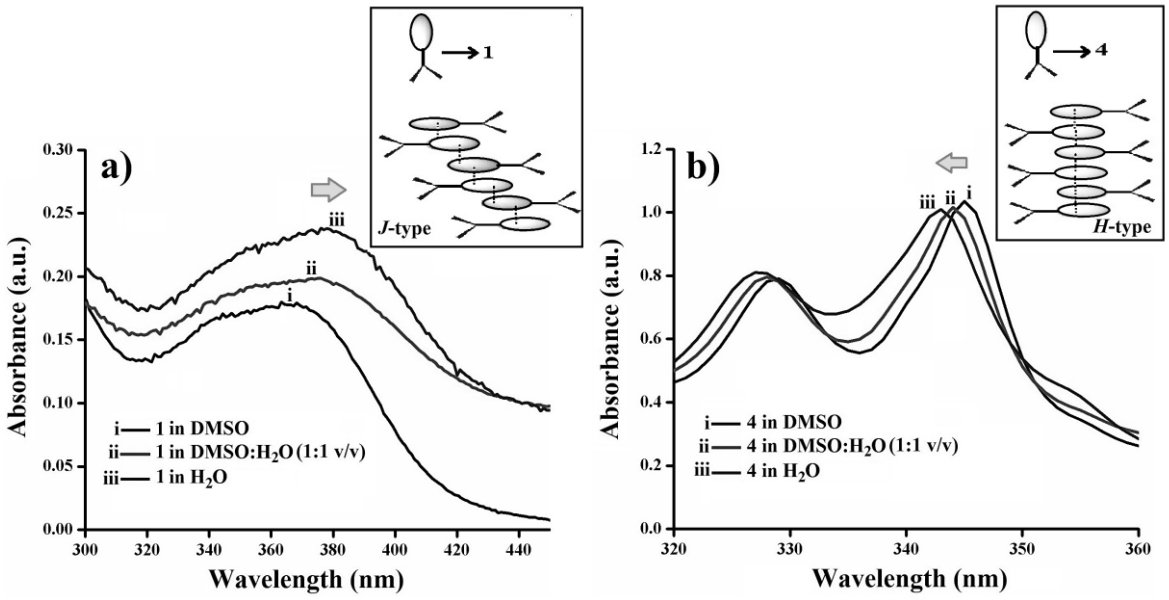

Figure 7. UV-Vis spectra of (a) ANS tagged gelator-**1** and (b) native gelator-**4** in different solvents.

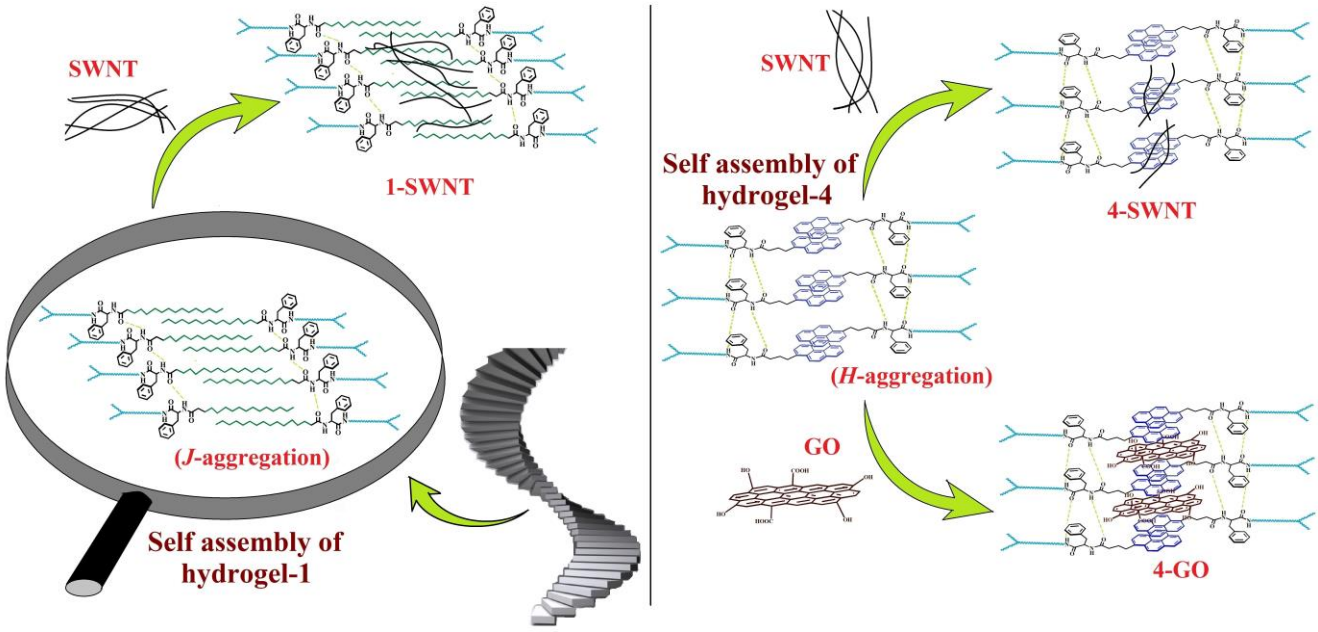

Figure 8. Pictorial representation of the self-assembly of hydrogel-**1** and -**4** and inclusion of SWNT and GO.

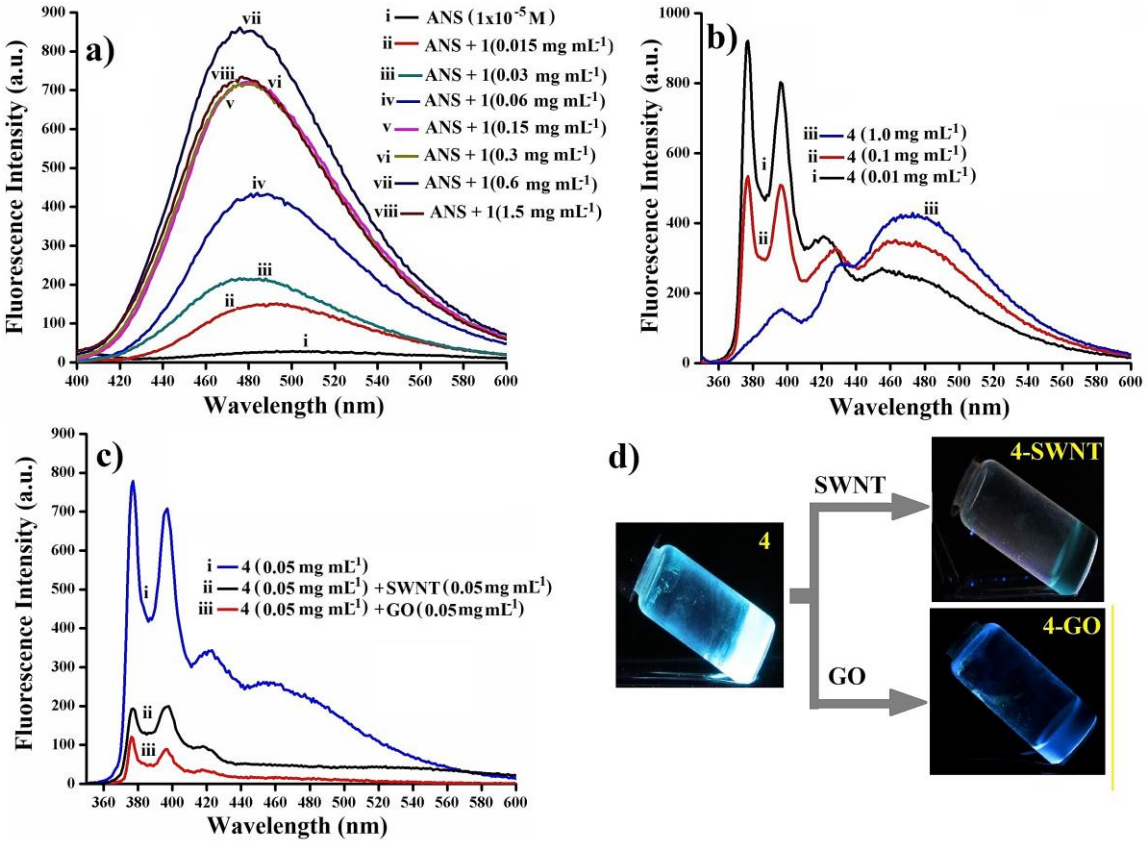

Figure 9. Fluorescence spectra of (a) **1** and (b) **4** with varying concentrations. (c) Fluorescence quenching of **4** upon inclusion of SWNT and GO within the self-assembly. Photographic images of (d) **4**, **4**-SWNT and **4**-GO upon irradiation with UV torch.

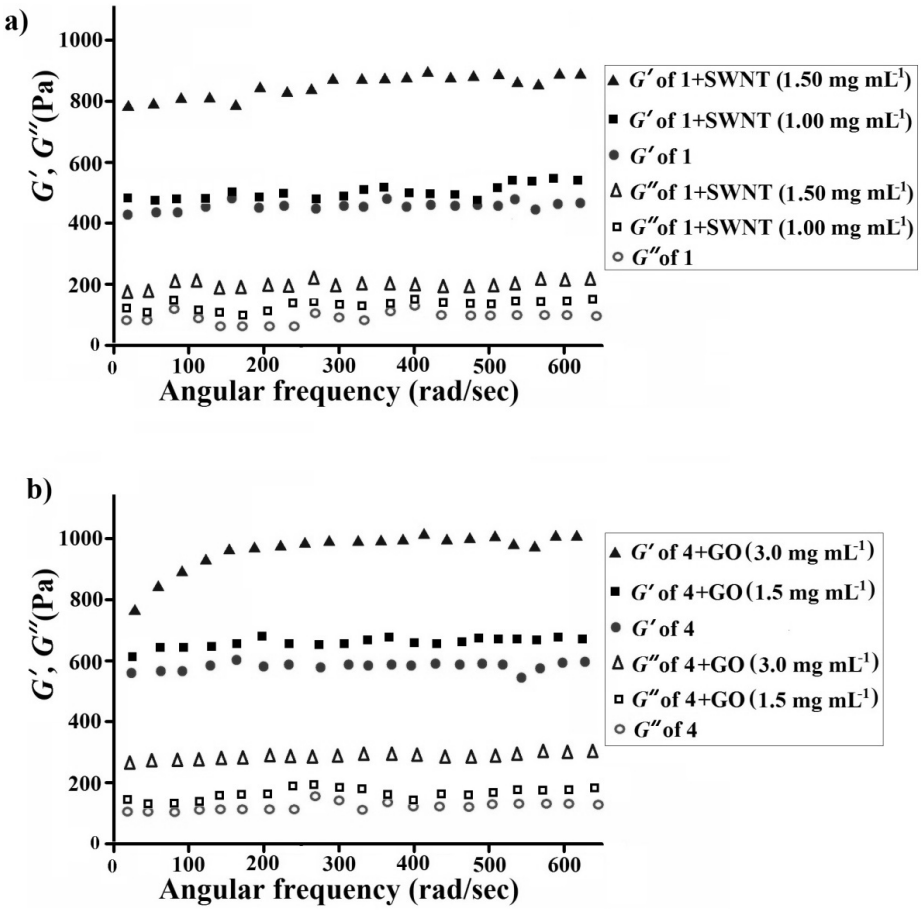

Figure 10. Plots of *G′* and *G″* of (a) hydrogel-**1** and **1**-SWNT and (b) hydrogel-**4** and **4**-GO.

Graphical Abstract

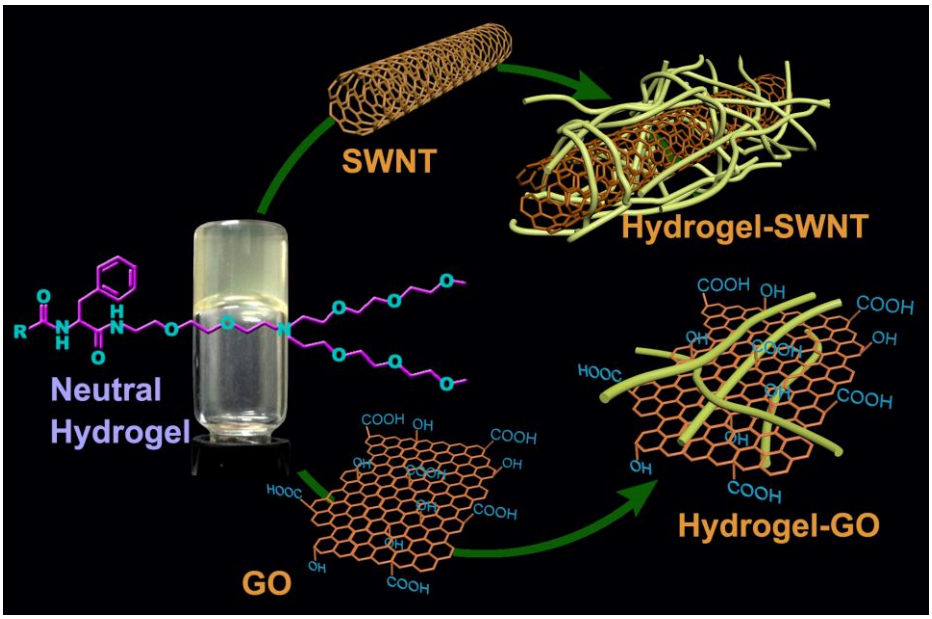

L-phenylalanine containing triethylene glycol monomethyl ether tagged neutral hydogelators were developed with variation in the hydrophobicity from C-16 alkyl chain to extended aromatic moiety, pyrene. Gelator's structure dependent inclusion of carbon nanomaterials (CNMs) of different dimension within the gel matrix was investigated. Long chain C-16 containing gelator can include 1D allotrope of carbon (SWNT) while pyrene containing gelator with additional π-π stacking interaction can incorporate both 1D (SWNT) and 2D (GO) allotrope of carbon within its self-assembled fibrillar network. Distinctive self-aggregation pattern of the gelators through *J*- and *H*-type self-assembly possibly played a key role in successful integration of CNM of different dimensions within the hydrogels.

Keywords: Amphiphile, carbon nanomaterials, hydrogel, neutral gelator, self-assembly, soft-nanocomposite